Comparison of Analysis of Linear Inhomogeneous and Nonlinear Half-Space in Foundation-Subsoil Interaction

J. Labudkova and R. Cajka

***Abstract*—**The solution of tasks of interaction of foundation and subsoil is more difficult the less accurate the input data. Lower accuracy of input data is related to the description of the properties and behavior of foundation soil. Foundation soil consists of heterogeneous particles. The modulus of deformability in the subsoil model varies smoothly with increasing depth. It was resolved by use of an inhomogeneous half-space. The other alternative, besides linear inhomogeneous half-space, is nonlinear analysis. The results of both alternatives of solutions are compared in this paper. Values calculated by interaction models bases on FEM with 3D elements of subsoil were also compared with values measured during the loading test.

***Keywords*—**3D FEM Elements, Contact Stress, Foundation structure, Soil–Structure Interaction.

I. Introduction

At present there is no generally valid model of subsoil. As a consequence the results of the solution may be different. This is caused by dependence on the choice of the model subsoil. Interaction models are gradually improving. The subsoil can be modeled as a 2D model of the surface of subsoil or as a 3D model of the soil massif. The 3D model of the soil massif allows a detailed description of processes running inside the subsoil. The 3D model of the subsoil can be created as a half-space. The half-space is a continuum bounded from above by a plane. The models of the subsoil and subsoil-structure interaction are also dealt with in [5, 12, 13, 14, 16, 18, 24].

An elastic homogeneous isotropic continuum is the simplest idealization of the half-space. It is composed of a substance for which Hooke's law is valid. The properties of the continuum depend on two material parameters. These parameters are the elastic modulus and Poisson's ratio. The size of the modeled area representing the subsoil, choice of boundary conditions and the size of the finite-element mesh are difficult to determine correctly, especially if the model of the subsoil consists of 3D finite elements [9, 10, 23, 26].

Foundation soil is a heterogeneous material. Its properties are therefore different from the idealization of linear elastic isotropic homogeneous material. That is why the calculated values do not correspond to the values of settlement measured for real buildings or during the experiments. Other experimental measurements associated with subsoil-structure interaction are also dealt with in [1, 2, 4, 7, 11, 17, 19].

Use of the model of inhomogeneous half-space or nonlinear calculation is a possible way to a more accurate capturing of the real behavior of the subsoil.

II. Linear inhomogeneous half-space

The modulus of elasticity of the modeled area representing the subsoil varies smoothly with increasing depth.

Concentration of the vertical stress in the axis of the foundation placed on the inhomogeneous half-space is different in comparison with the homogeneous half-space. The relationship based on conditions of low deformation work was derived by Frölich [21]. The modulus of elasticity increases linearly with depth [21]:

$$E_{def} = E_0 z^m \tag{1}$$

$$m = \frac{1}{\mu} - 2 \tag{2}$$

where

E_0 – modulus of deformability at the surface

z – z-coordinate (depth)

m – coefficient depending on Poisson's ratio μ

III. Nonlinear half-space

Structural and physical nonlinearity were applied in the performed FEM analysis. Another FEM analysis associated with subsoil-structure interaction and its results are also dealt with in [6, 10].

Foundation-subsoil interaction is a contact task. The calculation is always performed by nonlinear analysis due to structural nonlinearities. This structural nonlinearity is induced by unilateral bond. This unilateral bond acts exclusively in

This outcome has been achieved with the financial support by Student Grant Competition VSB-TUO. Project registration number is SP2015/108.

Jana Labudkova, Faculty of Civil Engineering, Department of Structures, VSB – Technical University Ostrava, Czech Republic, e-mail: jana.labudkova@vsb.cz, telephone: 00420 597 321 925, (corresponding author).

Radim Cajka, Faculty of Civil Engineering, Department of Structures, VSB – Technical University Ostrava, Czech Republic, e-mail: radim.cajka@vsb.cz, telephone: 00420 597 321 344.

pressure (Fig. 1). The nonlinear analysis requires an iterative solution.

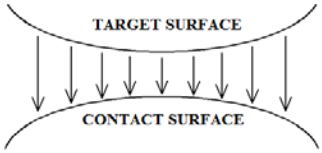

Fig. 1 Unilateral bond, contact task

Physical nonlinearity is associated with material properties. The nonlinear material model was performed by application of Drucker-Prager model. Behavior of the subsoil can be better described due the Drucker-Prager model.

In nonlinear analysis Hooke's law does not apply and exceeding of conditions of plasticity leads to lasting deformations. Fig. 2 shows the elastic-plastic material behavior during uniaxial stress and the creation of plastic deformations.

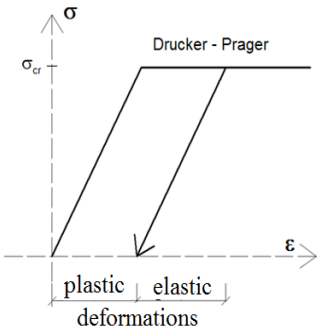

Fig. 2 Drucker-Prager model, elastic-plastic material

The Drucker-Prager model is derived from the condition of plasticity according to von Mises. The Drucker-Prager model is used for cohesive materials with internal friction. The Drucker-Prager model approximates to Mohr-Coulomb's plasticity condition (Fig. 3-a). Because of this, it is possible to describe the difference between the tensile and compressive strength (Fig. 3). The Drucker-Prager model has a smooth curve of limit stress in contrast to Mohr-Coulomb's condition of plasticity. This is advantageous in terms of numerical calculations. The nonlinear tasks and conditions of plasticity are described in greater detail in [6].

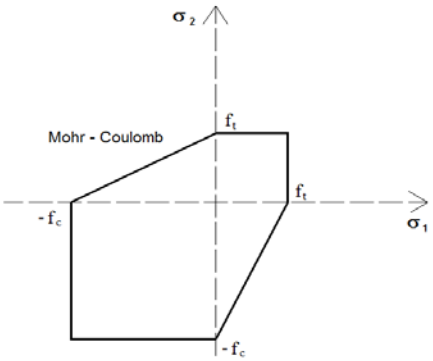

Fig. 3-a Mohr- Coulomb condition of plasticity

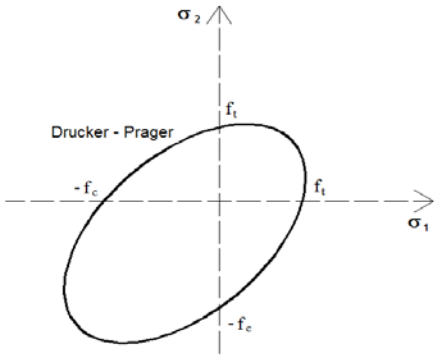

Fig. 3-b Drucker-Prager condition of plasticity

The nonlinear model is defined by the modulus of elasticity E, Poisson coefficient μ, internal friction angle φ[°], soil cohesion c [kPa] and dilatancy angle ψ [°].

IV. Implementation of the Numerical 3D Models in FEM Analysis

Input data required for numerical solution were taken from measurements obtained during the load testing [22]. The test sample was a prefabricated concrete tile (Fig. 4). A concrete tile was chosen because of simplicity of the experiment performed for verification of testing methods and equipment.

Fig. 4 Load testing of the slab

The dimensions of the concrete slab were 500x500x48mm. The class of concrete strength was C45/55. The top layer of subsoil consisted of loess loam, and its consistency class was F4. Its thickness was about 5m. The slab was loaded in the centre. The dimensions of the loaded area were 100x100mm. The load value was 18.640kN at the time of the failure of the slab (Fig. 5).

Fig. 5 Failure of the slab

A. 3D numerical models

The subsoil-structure interaction was resolved using numerical modeling in ANSYS 15.0.

The computational model was created by using the finite element SHELL 181 (2D) for the concrete slab. The 3D model of the subsoil was created by using the finite element SOLID 45 (3D). The finite element SHELL 181 was additionally defined by the thickness of the slab. The thickness was 48 mm.

Contact was mediated by contact pair TARGE 170–CONTA 173. The influence of friction between the slab and the subsoil was neglected at the contact area. The coefficient of friction was thus zero. Verification of directions of the normals on the contact surfaces was necessary. Normals must be directed against each other. If they are not, the rotation of these normals is necessary.

The model of the slab was loaded in the center on an area of 100x100mm. The uniform load corresponded to the value measured at the moment of the failure of the slab.

The horizontal and vertical shifts of the external walls (representing the subsoil area) were hindered by boundary conditions (Fig. 6).

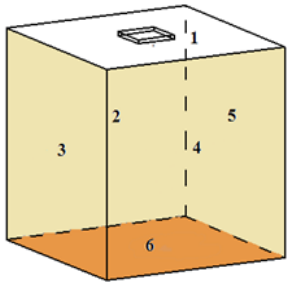

Fig. 6 Boundary conditions

B. Linear inhomogeneous half-space

Material No. 1 was marked concrete with modulus of elasticity E=36.3GPa and Poisson coefficient of μ=0.2. The model of the subsoil was created as a cube with dimensions 2.5x2.5x2.5m. The model was created as layered continuum consisting of 21 layers. The thickness of one layer was 0.125 m. The subsoil was marked as a material number 2-22 and the Poisson's ratio μ=0.35. Inhomogeneity of the subsoil was taken into account by increasing the value of modulus of deformability. The modulus of deformability began on the surface of the model. Its initial value was E_{def}=2.65 MPa. Its value progressively increased in deeper layers according to the formula:

$$E_{def} = E_o z^m \quad (Fig.7) \tag{3}$$

$$m = \frac{1}{\mu} - 2 = \frac{1}{0.35} - 2 = \underline{\underline{0.857}} \tag{4}$$

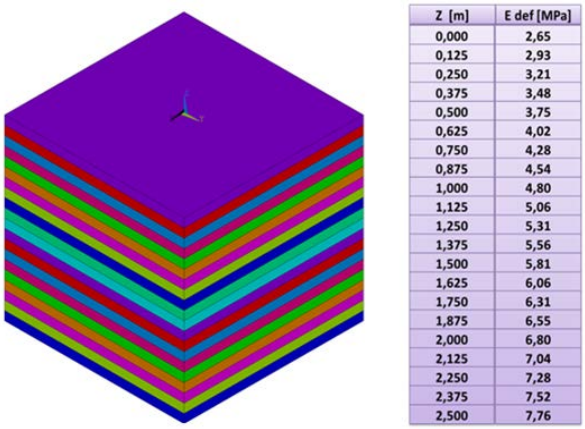

Z [m]	E def [MPa]
0,000	2,65
0,125	2,93
0,250	3,21
0,375	3,48
0,500	3,75
0,625	4,02
0,750	4,28
0,875	4,54
1,000	4,80
1,125	5,06
1,250	5,31
1,375	5,56
1,500	5,81
1,625	6,06
1,750	6,31
1,875	6,55
2,000	6,80
2,125	7,04
2,250	7,28
2,375	7,52
2,500	7,76

Fig. 7 Layers of the inhomogeneous half-space

The results of the FEM analysis are shown in following figures. Fig. 8 shows total deflection. The influence of boundary conditions is evident. Fig. 8 shows the total deformation in the vertical section through the subsoil model.

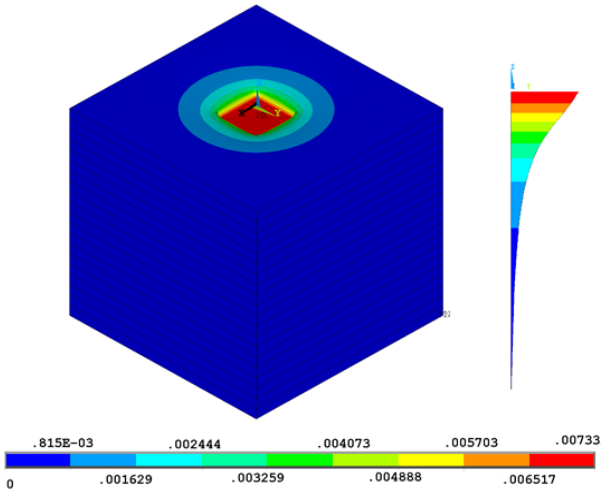

Fig. 8 Total deflection; vertical section in subsoil [m]

Fig. 9 shows the vertical component of the stress σ_z in the subsoil. The red areas show the tensile stress in the subsoil in the area of the settlement trough.

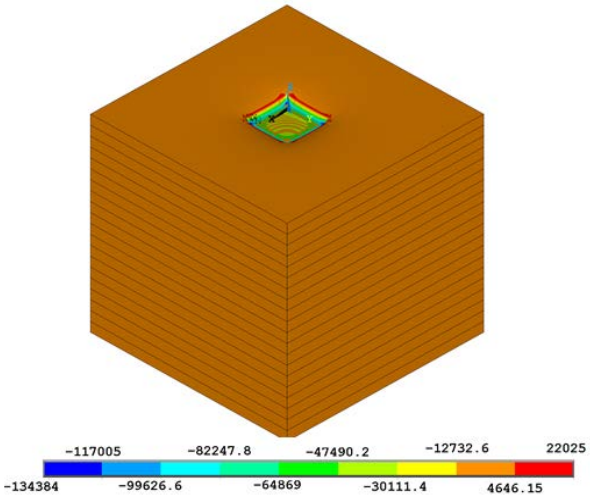

Fig. 9 Vertical component of the stress σ_z [Pa]

Distribution of the contact stress is shown in Fig. 10. According to the assumption there is a concentration of contact stress around the edge of the concrete slab and in the corners, where the contact stress is increased.

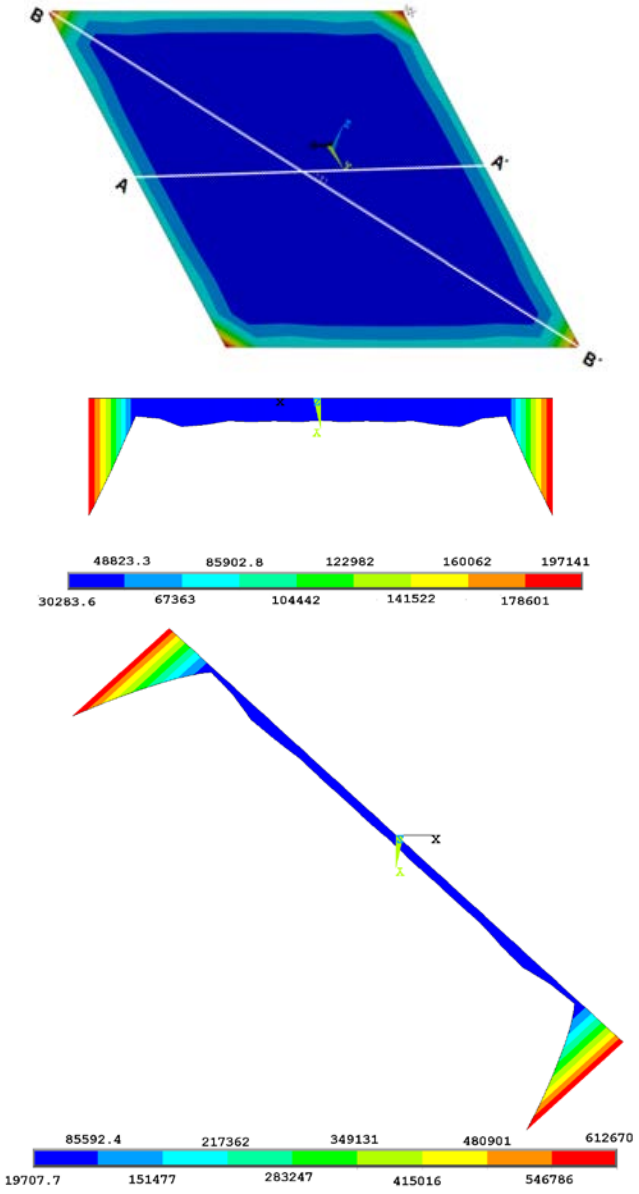

Fig. 10 Concentration of contact stress [Pa]

C. *Nonlinear half-space*

The model of the subsoil was created as a cube with dimensions 2.5x2.5x2.5m. Its finite-element mesh had a size of 0.05x0.05x0.05m. In reality, the subsoil is also capable of transmitting a lesser extent of tensile stresses. The use of the Drucker-Prager model corresponds well with this assumption. The Drucker-Prager model enables tensile stresses in material like subsoil.

The cohesion of the subsoil was c=15kPa and the internal friction angle was φ=25°. These values correspond to the characteristics of the soil classified as F4.

The results of FEM analysis are shown in the following figures. Fig. 11 shows total deflections.

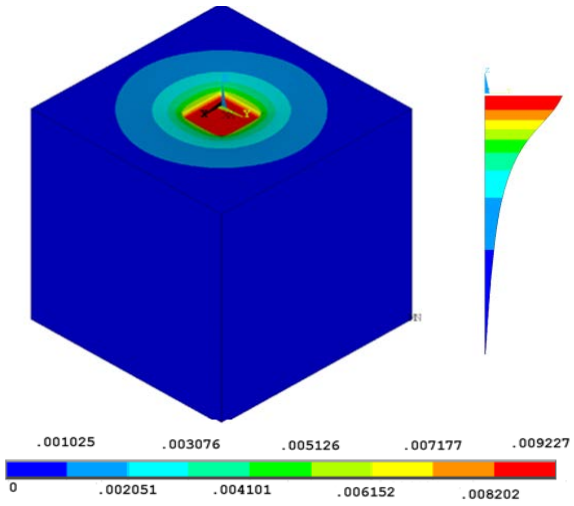

Fig. 11 Total deflection; vertical section in subsoil [m]

Plastic deformations originated under the corners of the slab after nonlinear analysis (Fig. 12). Plasticization has occurred. Tensile stress in the subsoil decreased after plasticization.

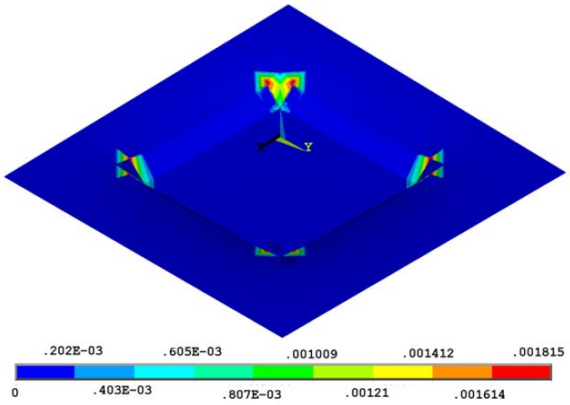

Fig. 12 Plastic deformations [m]

Fig. 13 shows the vertical component of the stress σ_z in the subsoil. Red areas show the tensile stress in the subsoil in the area of the settlement trough.

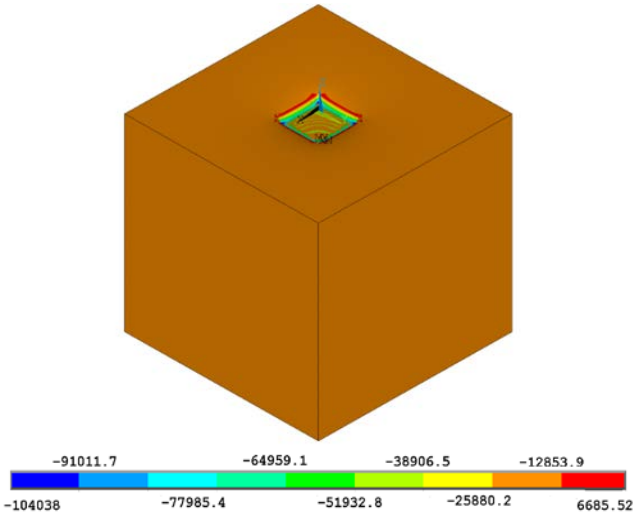

Fig. 13 Vertical component of the stress σ_z [Pa]

Distribution of the contact stress is shown in Fig. 14. According to the assumption there is a concentration of contact stress around the edge of the concrete slab and in the corners, where the contact stress is increased.

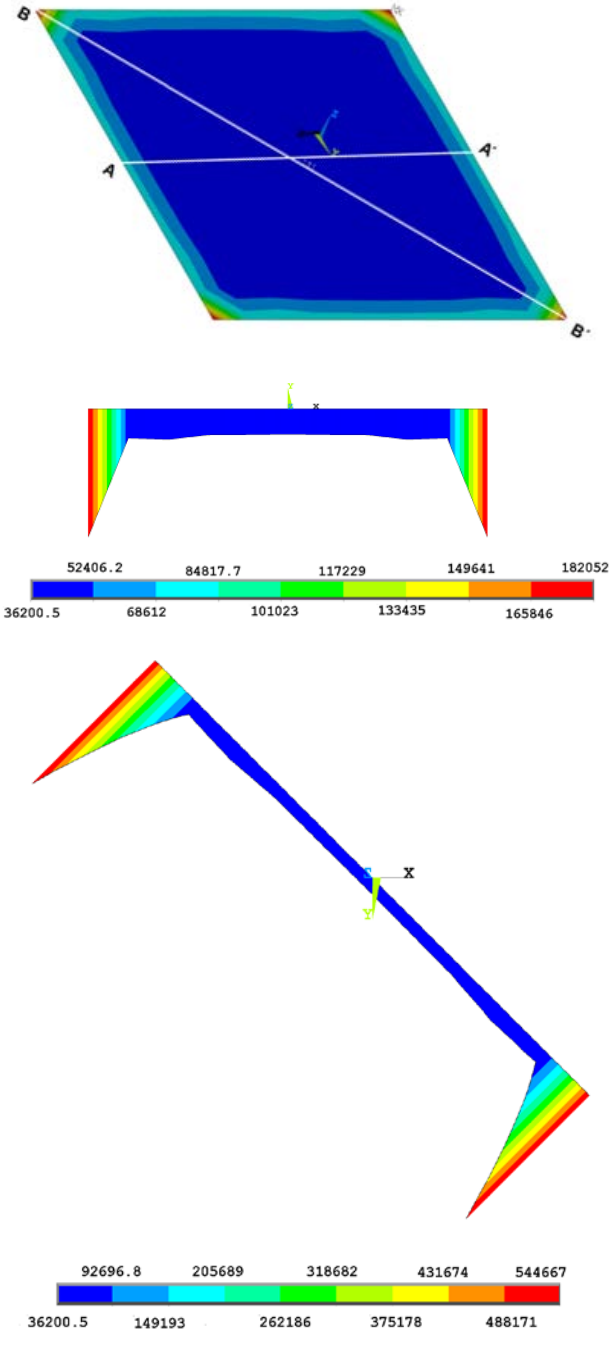

Fig. 14 Concentration of contact stress [Pa]

V. Parametric Study

Parametric study was performed. The resulting vertical deformations are affected by depth of the subsoil model. Subsoil model properties which depend on increasing depth are different in homogeneous half-space model and inhomogeneous half-space model. Influence of depth of nonlinear homogeneous half-space model and linear inhomogeneous half-space model was observed in this parametric study. The resulting vertical deformations are also affected by the boundary conditions. Three variants of boundary conditions were used in the parametric study (Fig. 15).

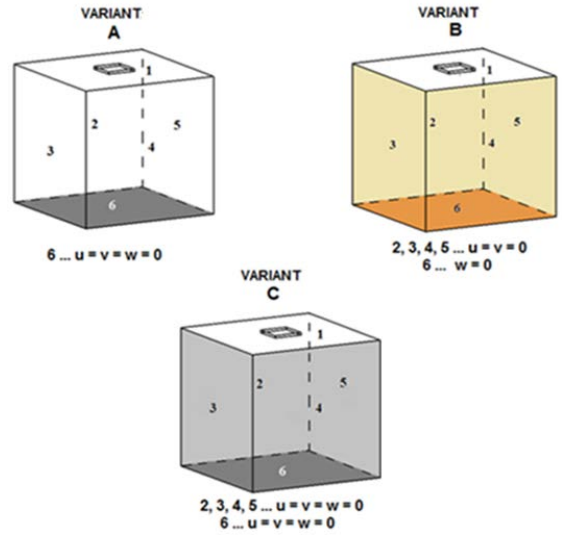

Fig. 15 Variants of boundary condition

Boundary conditions of variant A hinder the vertical and horizontal shifts in the lower base of the model (In Fig. 15 indicated by No. 6). No boundary conditions do not hinder nodes shifts of the peripheral walls of the model (these walls are marked by No. 2, 3, 4, 5 in Fig. 15). No boundary conditions do not hinder nodes shifts of the upper level of the subsoil model. Upper level of the subsoil model represents the terrain (In Fig. 15, marked by No. 1). Boundary conditions of variant B hinder the horizontal nodes shifts of the peripheral walls of the model (these walls are marked by No. 2, 3, 4, 5 in Fig. 15).

Boundary conditions of variant B hinder the vertical nodes shifts in the lower base of the model (In Fig. 15 indicated by No. 6). No boundary conditions do not hinder nodes shifts of the upper level of the subsoil model. Upper level of the subsoil model represents the terrain (In Fig. 15, marked by No. 1).

Boundary conditions of variant C hinder the vertical and horizontal nodes shifts of the peripheral walls of the model (these walls are marked by No. 2, 3, 4, 5 in Fig. 15). and also in the lower base of the model (In Fig. 15 indicated by No. 6). No boundary conditions do not hinder nodes shifts of the upper level of the subsoil model. Upper level of the subsoil model represents the terrain (In Fig. 15, marked by No. 1). The following graphs are created from parametric studies.

Comparison of deformations of nonlinear homogeneous half-space model and linear inhomogeneous half-space model is shown in the following graphs. All variants of boundary conditions were used in the models of a homogeneous half-space and in models of inhomogeneous half-space.

Fig. 16 shows the dependence of the slab deformations on the variable depth of the inhomogeneous subsoil model. The same ground area of the subsoil model (2.5x2.5m) was kept. Depth of subsoil model was growing always about 1.0 m (0.5 m, 1.5 m, 2.5 m).

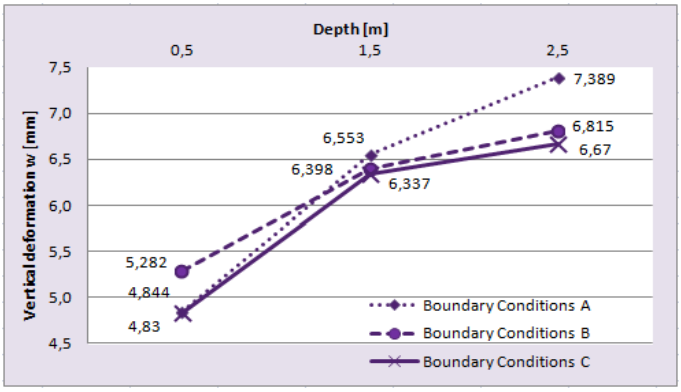

Fig. 16 Settlement of linear inhomogeneous half-space for all variants of boundary conditions

Fig. 17 shows the comparison of the slab deformations according to the variable depth of the nonlinear homogeneous subsoil model (dashed) and linear inhomogeneous subsoil model (fully) for boundary conditions of variant A.

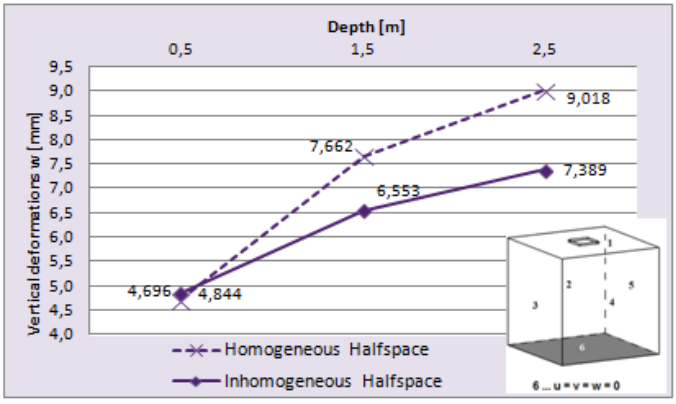

Fig. 17 Comparison of homogeneous subsoil model and inhomogeneous subsoil model, boundary conditions variant A.

Fig. 18 shows the comparison of the slab deformations according to the variable depth of the nonlinear homogeneous subsoil model (dashed) and linear inhomogeneous subsoil model (fully) for boundary conditions of variant B.

Parametric study for boundary condition of variant B is also shown by figures in the Table 1 and Table 2. Table 1 shows the percentage differences between the slab deformations on a homogeneous subsoil model with increasing depth of model. Table 2 shows the percentage differences between the slab deformations on an inhomogeneous subsoil model with increasing depth of model. Percentage differences between the slab deformations on homogeneous subsoil model and inhomogeneous subsoil model are also shown in Table 1 and Table 2.

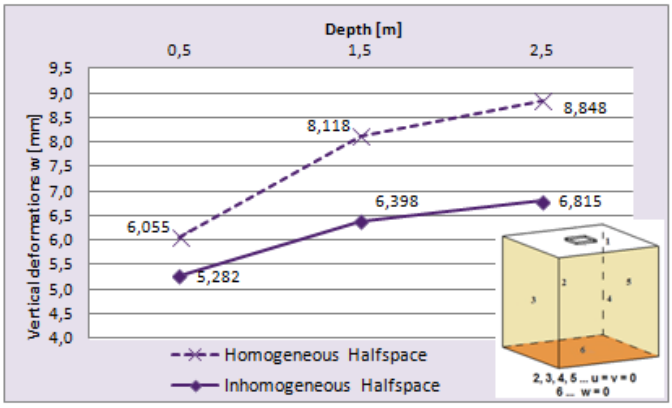

Fig. 18 Comparison of homogeneous subsoil model and inhomogeneous subsoil model, boundary conditions variant B.

Fig. 19 shows the comparison of the slab deformations according to the variable depth of the nonlinear homogeneous subsoil model (dashed) and linear inhomogeneous subsoil model (fully) for boundary conditions of variant C.

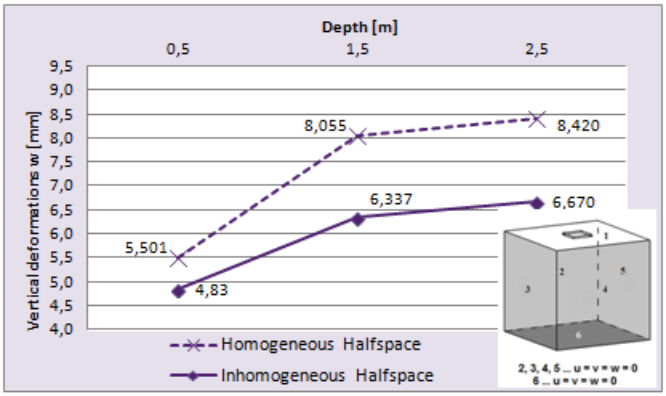

Fig. 19 Comparison of homogeneous subsoil model and inhomogeneous subsoil model, boundary conditions variant C

Fig. 20 shows the comparison of slab deformations according to the variable depth of the nonlinear homogeneous subsoil model (light) and linear inhomogeneous subsoil model (dark) for all variants of boundary conditions.

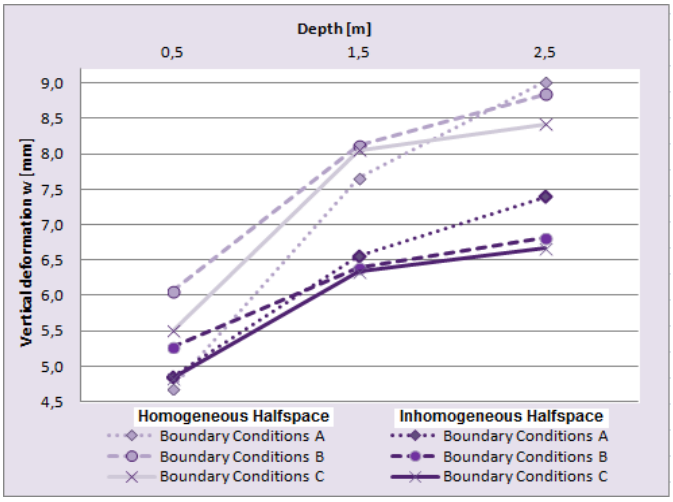

Fig. 20 Comparison of homogeneous subsoil model and inhomogeneous subsoil model, all boundary conditions.

Table 1 Settlement of nonlinear homogeneous half-space, variant of boundary conditions B

Table 2 Settlement of linear inhomogeneous half-space, variant of boundary conditions B

	NONLINEAR HOMOGENEOUS HALF-SPACE	LINEAR INHOMOGENEOUS HALF-SPACE
DEPTH h=0.5m	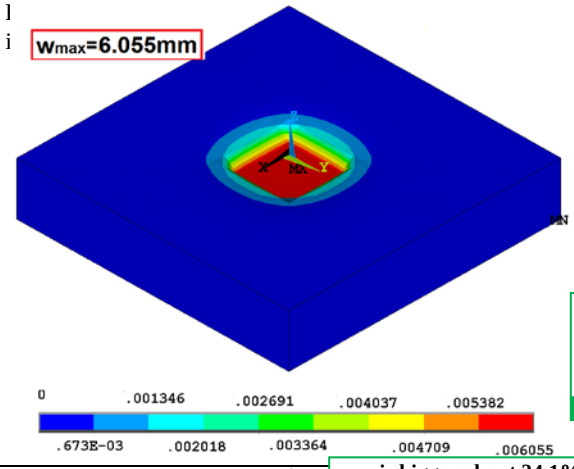	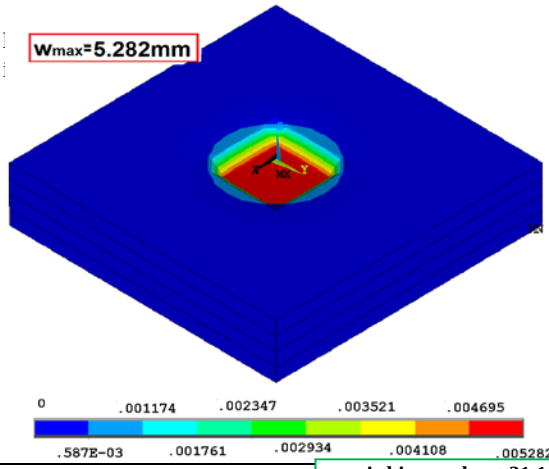
	wmax is smaller about 12.77%	
	wmax is bigger about 34.1%	wmax is bigger about 21.1%
DEPTH h=1.5m	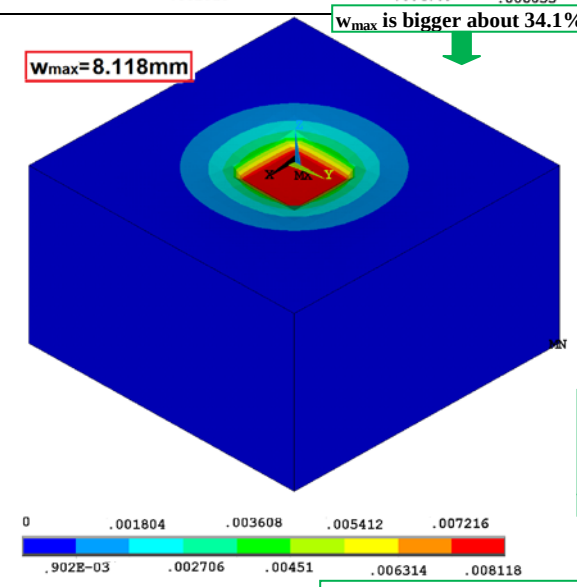	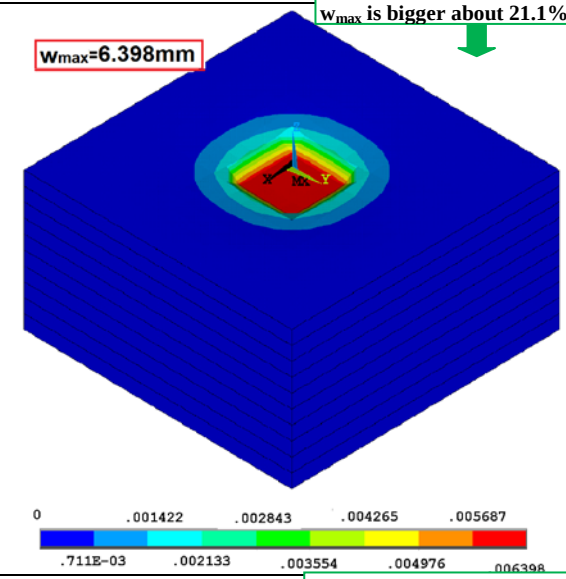
	wmax is smaller about 21.19%	
	wmax is bigger about 9.0%	wmax is bigger about 6.5%
DEPTH h=2.5m	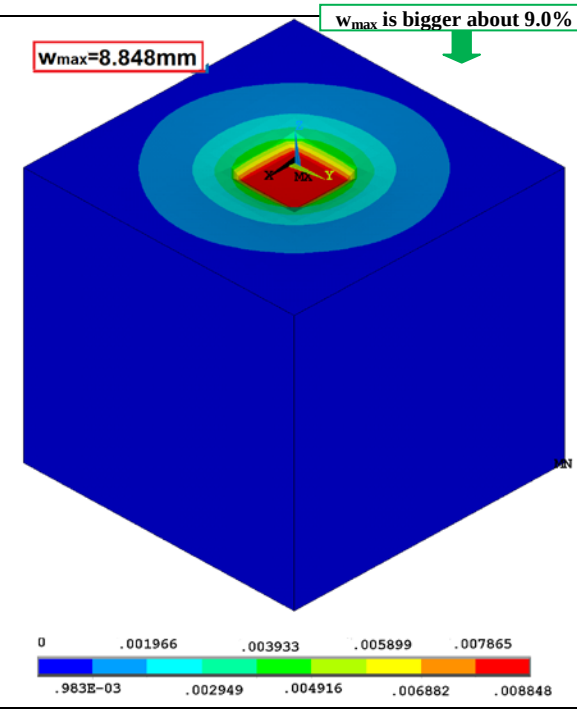	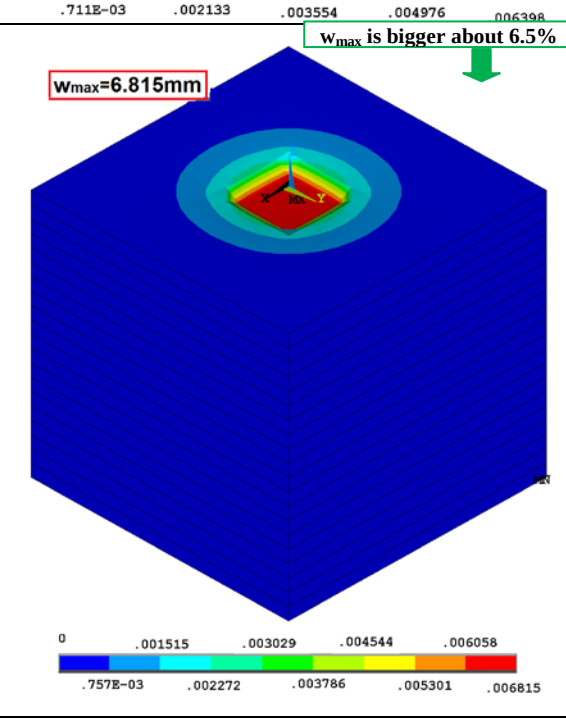
	wmax is smaller about 22.98%	

VI. Conclusion

A FEM analysis was performed for the model of linear inhomogeneous and nonlinear half-space. The maximum vertical deformation in the middle of the slab calculated by model of linear inhomogeneous half-space was 7.33mm. The maximum vertical deformation in the middle of the slab calculated by model of nonlinear half-space was 9.23mm. The difference is more than 25% between results of both compared analyses. During the experiment there was measurement of deformation in the middle of the plate about 3.5mm. The resulting deformation obtained by analysis of linear inhomogeneous half-space is closer to the real value of deformation. There can be many different reasons for deviations between the calculated and measured magnitude. For example, uncertainties associated with the determination of geomechanical properties of subsoil or climatic influences.

Analysis of the inhomogeneous linear continuum provides smaller vertical deformations than the model of the homogeneous nonlinear continuum. The reason is the modulus of deformability increasing with depth.

Plastic deformations originated under the corners of the slab after nonlinear analysis. It influenced the calculated pressure and tensile stresses. The maximum value of the compressive stress calculated by model of linear inhomogeneous half-space was 134.384 kPa. The maximum value of the compressive stress calculated by model of nonlinear half-space was 104.038kPa. The difference is more than 22%. Tensile stresses in the subsoil show greater difference. The maximum value of the tensile stress calculated by model of linear inhomogeneous half-space was 22.025kPa. The maximum value of the tensile stress calculated by model of nonlinear half-space was 6.685 kPa. The difference is more than threefold.

Percentage differences between the slab deformations on nonlinear homogeneous subsoil model and linear inhomogeneous subsoil model were shown. Slab deformations on linear inhomogeneous subsoil model are from 12.77% to 22.98% smaller than slab deformations on linear homogeneous subsoil model. Slab deformations increase about 34.1% between nonlinear homogeneous subsoil model with depth h=0.5m and h=1.5m. For linear inhomogeneous subsoil model an increase of the slab deformations is only 21.1%. Slab deformations increase about 9.0% between nonlinear homogeneous subsoil model with depth h=1.5m and h=2.5m. For linear inhomogeneous subsoil model an increase of the slab deformations is only 6.5%.

The results obtained in the analysis of inhomogeneous continuum are affected to a far smaller extent by the choice of the geometry and dimensions of the subsoil model. It follows that the use of inhomogeneous continuum provides more stable and usable results. The desirability of using the inhomogeneous continuum will be verified in further numerical modeling of the subsoil-structure interaction.

References

[1] M. Aboutalebi, A. Alani, J. Rizzuto, D. Beckett, "Structural behaviour and deformation patterns in loaded plain concrete ground-supported slabs," Structural Concrete. Vol. 15, No. 1, 2014, pp. 81-93.

[2] A. Alani, M. Aboutalebi, "Analysis of the subgrade stiffness effect on the behaviour of ground-supported concrete slabs," Structural Concrete, Vol. 13, No. 2, 2012, pp. 102-108.

[3] R. Cajka, M. Krejsa, "Measured Data Processing Using the DOProC Method," Advanced Materials Research, Vol. 859, 2014, pp 114-121, Trans Tech Publications, Switzerland.

[4] R. Cajka, K. Burkovic, V. Buchta, R. Fojtik, "Experimental Soil – Concrete Plate Interaction Test and Numerical Models," Key Engineering Materials, Vols. 577-578, 2014, pp 33-36 Trans Tech Publications, Switzerland.

[5] R. Cajka, "Horizontal friction parameters in soil-structure interaction tasks," Advanced Materials Research, Vol. 818, 2013, pp. 197-205.

[6] R. Cajka, P. Manasek, "Finite element analysis of a structure with a sliding joint affected by deformation loading," Proceedings of the 11th International Conference on Civil, Structural and Environmental Engineering Computing, Civil-Comp, 2007, 18p.

[7] R. Cajka, K. Burkovic, V. Buchta, "Foundation Slab in Interaction with Subsoil," Advanced Materials Research, Vols. 838-841, 2014, pp 375-380, Trans Tech Publications, Switzerland.

[8] R. Cajka, "Numerical Solution of Temperature Field for Stress Analysis of Plate Structures," Applied Mechanics and Materials, Vol. 470, 2014, pp 177-187. Trans Tech Publications, Switzerland.

[9] J. Labudkova, R. Cajka, "Comparison of Measured Deformation of the Plate in Interaction with the Subsoil and the Results of 3D Numerical Model," Advanced Materials Research, Vol. 1020, 2014, pp 204-209, Trans Tech Publications, Switzerland.

[10] R. Cajka, J. Labudkova, "Fibre Concrete Foundation Slab Experiment and FEM Analysis," Key Engineering Materials, Vols. 627, 2015, pp 441-444, Trans Tech Publications, Switzerland.

[11] V. Buchta, P. Mynarcik, "Experimental testing of fiberconcrete foundation slab model," Applied Mechanics and Materials, Vol. 501 – 504, 2014, pp. 291-294, Trans Tech Publications, Switzerland.

[12] K. Frydrysek, R. Janco, H. Gondek, "Solutions of Beams, Frames and 3D Structures on Elastic Foundation Using FEM," International Journal of Mechanics, Issue 4, Vol. 7, 2013, pp. 362-369.

[13] M. Janulikova, M. Stara, "Reducing the Shear Stress in the Footing Bottom of Concrete and Masonry Structures," Procedia Engineering, Vol. 65, 2013, pp. 284-289.

[14] J. Kralik, "Optimal design of NPP containment protection against fuel container drop," Advanced Materials Research, Vol. 688, 2013, pp. 213-221, Trans Tech Publications, Switzerland.

[15] J. Halvonik, L. Fillo, "The Maximum Punching Shear Resistance of Flat Slabs," Procedia Engineering, Vol. 65, 2013, pp. 376-381.

[16] T. Janda, M. Sejnoha, J. Sejnoha, "Modeling of soil structure interaction during tunnel excavation: An engineering approach," Advances in Engineering Software, pp. 51-60.

[17] R. Cajka, P. Mateckova, M. Janulikova, "Bitumen Sliding Joints for Friction Elimination in Footing Bottom," Applied Mechanics and Materials, Volume 188, (2012), pp. 247-252, ISSN: 1660-9336, ISBN: 978-303785452-5, 2012.

[18] H. Han, W. Bao, T. Wang, "Numerical simulation for the problem of infinite elastic foundation," Computer Methods in Applied Mechanics and Engineering, Vol. 147, Issue 3-4, 5 1997, pp. 369-385.

[19] X. Huang, X. Liang, M. Liang, M. Deng, A. Zhu, Y. Xu, X. Wang, Y.Li, "Experimental and theoretical studies on interaction of beam and slab for cast-in-situ reinforced concrete floor structure," Journal of Building Structures / Jianzhu Jiegou Xuebao, Vol. 34, 2013, No. 5, pp. 63-71.

[20] Janulikova, M. "Behavior of selected materials to create sliding joint in the foundation structure," Advanced Materials Research, Vol. 838-841, 2014, Pages 454-457.

[21] J. Feda, "State of stress in the subsoil and methods of computation of final settlement," Academia, 152 p, 1974. (in Czech)

[22] R. Cajka, V. Krivy, D. Sekanina, "Design and Development of a Testing Device for Experimental Measurements of Foundation Slabs on the Subsoil," Transactions of the VSB - Technical University of Ostrava, Construction Series, Volume XI, Number 1/2011, VSB - TU Ostrava, Pages 1–5, ISSN (Online) 1804-4824, ISSN (Print) 1213-1962.

[23] R. Cajka, J. Labudkova, "Dependence of deformation of a plate on the subsoil in relation to the parameters of the 3D model," International Journal of Mechanics, North Atlantic University Union, Volume 8, Pages 208-215, 2014, ISSN: 1998-4448.
[24] M. Janulikova, P. Mynarcik, "Modern Sliding Joints in Foundations of Concrete and Masonry Structures," International Journal of Mechanics, North Atlantic University Union, 2014, pp.184-189, ISSN: 1998-4448.
[25] M. Stara, V. Buchta, "Experimental tests of pre-stressed masonry and numerical modeling of resultant deformations," International Journal of Mechanics, North Atlantic University Union, 2014, pp. 138-143, ISSN: 1998-4448.
[26] R. Cajka, J. Labudkova, "Influence of parameters of a 3D numerical model on deformation arising in interaction of a foundation structure and subsoil," 1st International Conference on High-Performance Concrete Structures and Materials (COSTMA '13), Budapest, Hungary, 2013.